Acta Chemica Scandinavica A 31 (1977) 132—140

An X-Ray Diffraction Study of Iodide and Bromide Complexes of Mercury(II) in Aqueous Solution

MAGNUS SANDSTRÖM and GEORG JOHANSSON

Department of Inorganic Chemistry, Royal Institute of Technology, S-100 44 Stockholm 70, Sweden

From X-ray scattering measurements on concentrated aqueous solutions of the mercury(II) halides the Hg–X bond lengths in the tetrahedral HgX_4^{2-} complexes have been determined to be 2.785(3) Å for the iodide and 2.610(5) Å for the bromide. The X-ray scattering data are consistent with the formation of mononuclear HgI_3^- or $HgBr_3^-$ ions when the X/Hg mol ratio in the solutions is reduced below 4.0. The Hg–X bond lengths in the pyramidal HgI_3^- and $HgBr_3^-$ complexes are estimated to be about 0.03 Å shorter than in the corresponding HgX_4^{2-} complexes. A model for the hydration of the HgX_4^{2-} complexes, which is consistent with the scattering data, is suggested.

As part of a series of X-ray investigations of the structures of the mercury(II) halide complexes in different solvents, aqueous solutions of mercury(II) chloride, bromide and iodide have been investigated. The first paper in this series was a study of mercury(II) iodide complexes in DMSO solution.[1]

The low solubilities of the HgX_2 complexes in water do not allow accurate structure determinations of the lower halide complexes. The chloride solutions will be treated in the following paper.[2]

Previous work. Several investigations of the mercury(II) halide complexes in aqueous solutions, applying different methods,[3,4] have been reported in the literature. Emf measurements on dilute solutions have shown that HgX^+, HgX_2, HgX_3^- and HgX_4^{2-} complexes are formed.[5,6] The emf data give no evidence for the formation of polynuclear complexes at the low concentrations used. The stability constants show the ranges of stability of the iodide and bromide complexes to be well separated (Fig. 1), which allows the preparation of solutions in which a specific complex can be dominant.

From X-ray scattering measurements on approximately 1 M solutions of mercury(II) with sodium iodide and bromide, van Eck [7,8] concluded from the positions of peaks in the radial distribution functions (RDF), that the HgX_4^{2-} ions are probably tetrahedral but highly distorted. Within an HgX_4^{2-} tetrahedron all Hg–X bonds were found to be equal, but

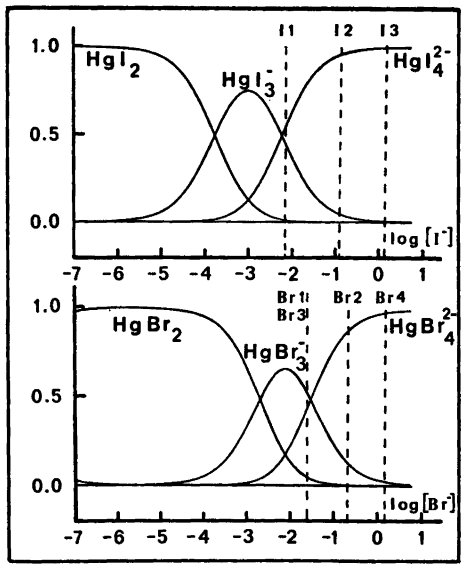

Fig. 1. Fraction of Hg bonded in the different halide complexes as a function of the free halide concentration. The calculated complex distributions of the solutions investigated, assuming the equilibrium constants to be valid, are indicated.

large differences seemed to occur between the X−X distances.[8] A similar investigation was carried out by Furey [9] on approximately 3 M mercury(II) iodide solutions. He concluded that the HgI_4^{2-} group is a regular tetrahedron with an Hg−I bond length of 2.80 Å. In a solution with an I/Hg ratio of 3.6, where HgI_3^- complexes should be present, he found the same tetrahedral coordination of iodide, which requires the sharing of iodide ions between mercury atoms.

Results from spectroscopic investigations support a regular tetrahedral structure for the HgX_4^{2-} complexes in solution.[10-12] In anhydrous TBP solutions Raman and IR spectra have been interpreted as indicating a planar symmetry for HgI_3^-. For $HgBr_3^-$ in TBP, however, a deviation from planarity occurred probably caused by solvent interactions.[13]

In DMSO X-ray scattering measurements have shown the HgI_2 complex to be approximately linear, HgI_3^- to have a pyramidal shape and HgI_4^{2-} to form a regular tetrahedron.[1]

EXPERIMENTAL

The solutions were prepared by dissolving dried and weighed amounts of mercury(II) halide and sodium halide (Mallinckrodt, analytical reagent) in distilled water and diluting to a known volume. The compositions of the solutions investigated are given in Table 1.

The X-ray scattering was measured (at 25 ± 1 °C) from the free surface of the solutions in the way described in previous papers.[15] Mo$K\alpha$ radiation (λ = 0.7107 Å) was used. The scattered intensity was measured at discrete points between θ = 1° and θ = 70°, where 2θ is the scattering angle. Intervals of 0.1° for 1° < θ < 10° and 0.25° for 10° < θ < 70° were used. Usually 100 000 counts were taken for each point, which corresponds to a statistical error of about 0.3 %.*

Table 1. Compositions of the solutions at 25 °C in mol l^{-1}.

Sol.	Hg	X	Na	H_2O
I1	3.453	12.20	5.297	27.89
I2	3.052	12.21	6.104	28.02
I3	2.693	12.18	6.792	28.63
Br1	1.923	6.520	2.675	44.61
Br2	1.630	6.521	3.261	44.62
Br3	3.600	12.21	5.010	34.58
Br4	2.700	12.21	6.809	34.93

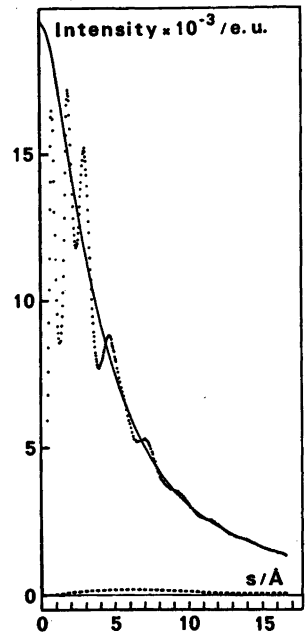

Fig. 2. Experimental normalized intensity values (dots), calculated structure-independent coherent scattering (line), and the incoherent scattering reaching the counter (dashed line), as a function of $s = (4\pi/\lambda) \sin\theta$ for solution I3.

DATA TREATMENT

All calculations were carried out by means of the KURVLR and PUTSLR programs.[16] The measured intensities were corrected and normalized to a stoichiometric unit of volume, V, corresponding to the average volume per mercury atom in the solution. The normalization was done by comparing the observed intensities with the calculated sum of the independent coherent and the incoherent scattering in the high angle region. The double scattering [17] was calculated and did not exceed 2 % for the iodide solutions and 3 % for the bromide solutions. The reduced intensities, $i(s)$, were obtained as described previously.[15]

* The intensity data can be obtained on request from the authors.

The scattering factors given by Cromer and Waber [18] were used for all the atoms except H, for which Stewart's values [19] were used. Anomalous dispersion corrections, $\Delta f'$ and $\Delta f''$, were taken from Cromer.[20] The values used for the incoherent radiation were those given by Cromer [21] for O, Br and I, by Compton and Allison [22] for H, and by Cromer and Mann [23] for the remaining atoms. Corrections were made for the Breit-Dirac factor,[24,25] in the form appropriate for a radiation counter.[26]

The reduced intensity curves, $i_{obs}(s)$, where $s = (4\pi/\lambda) \sin \theta$, were corrected for low-frequency additions by removing peaks in the RDF's below 1 Å, which could not be related to interatomic distances.[16] From the reduced intensity values the electronic radial distribution functions, $D(r)$, were calculated.[16] The modification function, $M(s)$, was $[f_{Hg}^2(0)/f_{Hg}^2(s)]$ exp $(-0.01s^2)$, and ϱ_0 was calculated as $[(\sum_p f_p)^2 + (\sum_p \Delta f_p'')^2]/V$.

Intramolecular contributions to the intensities were calculated according to the expression:

$$i_{calc}(s) = \sum_{\substack{p \\ p \neq q}} \sum_{q} (f_p f_q + \Delta f_p'' \Delta f_q'') [\sin (r_{pq}s)/(r_{pq}s)] \exp (-b_{pq}s^2)$$

Here r_{pq} is the average distance between the atoms p and q, and $b_{pq} = \frac{1}{2} \langle \Delta r^2 \rangle$ is a temperature coefficient, equal to half the mean square variation in r_{pq}. When the variation in r_{pq} is caused only by molecular vibrations, the amplitude of vibration equals Δr. Corresponding peak shapes were obtained from these intensities by a Fourier transformation carried out in the same way as for the experimental intensities. Intensity contributions from coordinated water molecules were calculated using the molecular scattering factor for H_2O, given by Narten.[27]

The experimental intensities obtained for solution I3 are illustrated in Fig. 2. For all the solutions the reduced intensities, after multiplication by s, are shown in Fig. 3. Radial distribution curves, $D(r)$ and $D(r) - 4\pi r^2 \varrho_0$, are given in Figs. 4 and 7.

Least squares refinements. Reduced intensities, i_{calc}, can be evaluated for assumed models of a solution, taking both intra- and intermolecular interactions into account.[16] The parameters defining such a model can be refined by minimizing the function $U = \sum w(s)[i_{obs}(s) - i_{calc}(s)]^2$, where $w(s)$ is a weighting function,[16,28] and the i_{calc} values are evaluated for each experimental point in a selected s interval.

Usually only the intramolecular interactions will give significant contributions to the high-angle part of the intensity curve, which can therefore be used for the refinement of the corresponding parameters.

An intramolecular interaction can be characterized by three parameters: the distance, r_{pq}, the number of such distances, n, in a stoichiometric unit of volume, and a temperature coefficient, b_{pq}. The result of a refine-

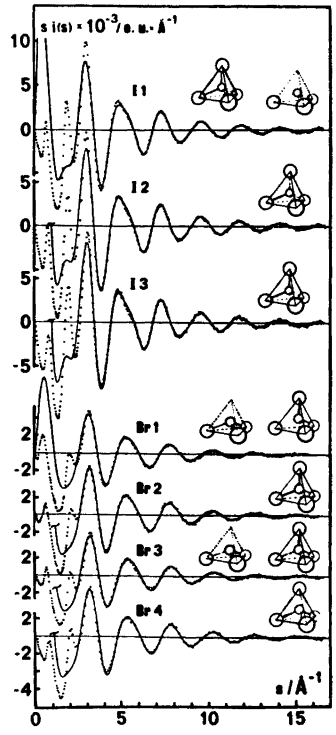

Fig. 3. Reduced intensity values, multiplied by s, (dots), for the solutions investigated. The solid lines give calculated $si(s)$ values for regular tetrahedral HgX_4^{2-} complexes with parameter values $b_{Hg-X} = 0.006$ Å^2, $b_{X-X} = 0.028$ Å^2, and $r_{Hg-X} = 2.785$ and 2.610 Å for the iodide and bromide solutions, respectively. For solutions I1, Br1 and Br3 stoichiometric amounts of pyramidal HgX_3^- complexes are also included, with $r_{Hg-X} = 2.76$ and 2.58 Å, respectively.

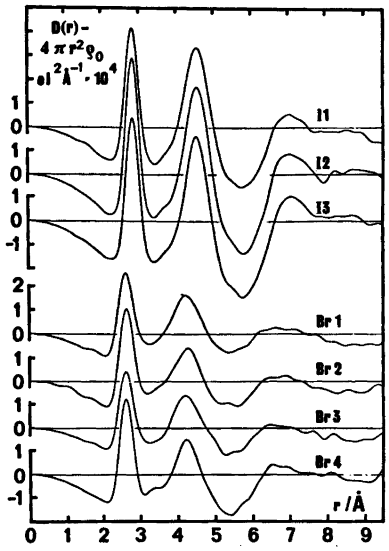

Fig. 4. $D(r)-4\pi r^2\varrho_0$ functions for the solutions investigated.

ment will be meaningful only if all the significant contributions to the reduced intensities in the selected s interval are included in the model.[28] Moreover, the number of parameters which can be simultaneously refined is small due to the limited amount of information which is contained in the one-dimensional intensity curve.

Systematic errors [15,17,28-35] which still can remain in the $i_{obs}(s)$ curve will in general have a much longer period in regard to s than those of the intramolecular interactions and will to a large extent be eliminated by the removal of spurious peaks at low distances in the RDF's.[16] A check for systematic errors can be made by comparing results obtained from refinements carried out for different s intervals. In particular, by varying the lower s limit, systematic errors caused by intermolecular intensity contributions can be detected as they decrease rapidly with increasing s values.

RESULTS

For all the solutions in the present investigation, the RDF's show only two prominent peaks (Fig. 4). One corresponds to the Hg–X and the other to the X–X distances within the mercury halide complexes. These interactions are by far the dominant contributors to the reduced intensity curves, with the exception of the innermost parts as is illustrated in Fig. 3. Therefore, accurate parameter values for these two types of intramolecular interactions can be determined by least squares refinements in which the low-angle parts of the intensity curves are not included.

A number of refinements were carried out using different weighting schemes and different s intervals and with various symmetry restrictions imposed on the allowed variations of the parameter values for the Hg–X and the X–X interactions. However, no significant differences between the results were found when i_{obs} values for $s > 3$ Å^{-1} were used. A summary of the results of the least squares refinements is given in Tables 2 and 3. The standard deviations are those calculated in the least squares refinement process and do not include systematic errors. From the variation of the results with the different ranges of s values used, it seems that the systematic errors in the parameter values can be of about the same order of magnitude as the calculated standard deviations. All the refinement results given in the tables were obtained using a weighting function chosen to give each part of the $i(s)$ curve a weight corresponding approximately to its statistical accuracy and included a factor which compensated for the unequal spacing between the points caused by the constant $\Delta\theta$ values used during the intensity measurements.[2]

The RDF's and calculated peak shapes for solutions I2 and Br2 are shown in Fig. 7.

DISCUSSION

Intramolecular interactions. A simultaneous refinement of all six parameters used to describe the Hg–X and the X–X interactions leads to the results given in Table 2. The parameters r, n and b of the Hg–X interaction and the X–X distance are those most accurately determined. For X/Hg ratios of four and larger the number of X atoms bound to each mercury atom is found, within the estimated errors, to be four as expected for a tetrahedral complex. Similarly, the ratio between the X–X and the Hg–X distances is not significantly different from that expected for a regular tetrahedral symmetry.

Table 2. Results of least squares refinements of six independent parameters for the Hg – X and X – X interactions; r is the distance, n the number of distances per mercury atom, and b the temperature coefficient. For a regular tetrahedron the calculated ratio r_{Hg-X}/r_{X-X} is $\sqrt{3/8} = 0.6124$.

Sol.	Ratio X/Hg	r_{Hg-X}/Å	n_{Hg-X}	b_{Hg-X}/Å²	r_{X-X}/Å	n_{X-X}	b_{X-X}/Å²	r_{Hg-X}/r_{X-X}
I1	3.53	2.774(2)	3.5(1)	0.005(1)	4.55(1)	6(1)	0.03(1)	0.610(2)
I2	4.00	2.786(2)	3.9(1)	0.006(1)	4.55(1)	8(1)	0.04(1)	0.612(2)
I3	4.52	2.786(2)	3.9(1)	0.005(1)	4.55(1)	7(1)	0.03(1)	0.612(2)
Br1	3.39	2.597(2)	3.2(1)	0.006(1)	4.22(2)	9(2)	0.05(1)	0.615(4)
Br2	4.00	2.613(2)	3.9(1)	0.005(1)	4.26(1)	7(1)	0.04(1)	0.613(2)
Br3	3.39	2.594(3)	3.2(1)	0.006(1)	4.26(2)	9(2)	0.05(1)	0.609(4)
Br4	4.52	2.608(3)	3.9(1)	0.005(1)	4.25(2)	8(1)	0.04(1)	0.614(4)

Table 3. Results of least squares refinements of four independent parameters assuming tetrahedral HgX_4 groups; r is the Hg – X distance, m the number of HgX_4 complexes in a stoichiometric unit of volume, and b the temperature coefficient.

Sol.	r_{Hg-X}/Å	m	b_{Hg-X}/Å²	b_{X-X}/Å²
I2	2.785(2)	0.99(1)	0.006(1)	0.029(1)
I3	2.785(2)	0.98(2)	0.005(1)	0.025(2)
Br2	2.614(2)	1.01(2)	0.007(2)	0.028(2)
Br4	2.605(2)	1.00(2)	0.006(3)	0.029(3)

The number of Hg – X bonds for the solutions with X/Hg mol ratios less than four is of the magnitude expected if an HgX_3^- complex is assumed to be formed. This indicates that sharing of halide atoms between different complexes does not occur, and that, therefore, polynuclear complexes are not formed. However, the level of significance in these comparisons is relatively low as shown by the standard deviations given in Table 2. Because of the small contributions to the intensity curves of the X – X, compared to the Hg – X interactions, the standard deviations obtained for the number of X – X distances are high (Table 2). This parameter, therefore, cannot be used to differentiate between HgX_4^{2-} and HgX_3^- complexes.

A comparison of the RDF's between the solutions with X/Hg ≥ 4 and those with X/Hg < 4, shows more clearly that polynuclear complexes are not formed in significant amounts. This is demonstrated in Fig. 5, which gives differences between the $D(r) - 4\pi r^2\varrho_0$ functions for the following pairs of solutions: I2 – I1, Br2 – Br1 and Br4 – Br3. The difference in areas of the Hg – X peaks corresponds to that expected if a mononuclear HgX_3^- complex is formed and peaks which could indicate the presence of polynuclear complexes, do not appear in the difference curves.

The results from the least squares refinements, given in Table 2, indicate a slight shortening of the Hg – X distances for X/Hg mol ratios below 4. By using the parameter values for the HgX_4^{2-} complexes, as given in Table 3, and assuming the relative amounts of HgX_3^- and HgX_4^{2-} to be given by the X/Hg mol ratios, estimates of the Hg – X bond lengths in HgX_3^- could be obtained from the distances in Table 2 and by least squares refinements on solutions I1, Br1 and Br3. The results indicated the Hg – I and the Hg – Br bond lengths in

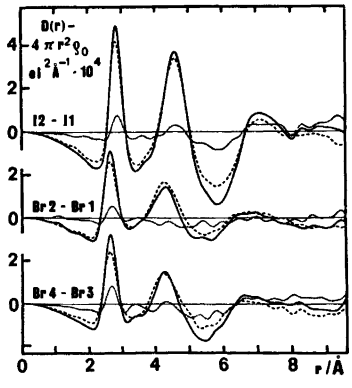

Fig. 5. Differences (dotted lines) between the $D(r) - 4\pi r^2\varrho_0$ functions for the solutions I2 – I1, Br2 – Br1, and Br4 – Br3.

HgX_3^- to be 0.03(1) Å shorter than those in HgX_4^{2-}. No shortening of the X–X distances, however, seems to occur. This is comparable to what was found for DMSO solutions,[1] where the Hg–I bond lengths were determined to be 2.80 and 2.73 Å in HgI_4^{2-} and HgI_3^-, respectively.

Table 3 gives the results of the refinements for solutions with X/Hg mol ratios ≥ 4, when only four of the six parameter values are allowed to vary independently. For this refinement a regular tetrahedral HgX_4 group was assumed to occur and the number of such groups in the stoichiometric unit of volume, the temperature factors corresponding to the Hg–X and the X–X interactions, and the Hg–X bond lengths were independently varied. Since the ratio between the number of X–X and Hg–X distances is constant in the complex, the precision in the determination of the temperature factor of the X–X interaction will be higher (Table 3). With this exception the parameter values given in Table 3 do not differ from those given in Table 2.

The temperature factor of the Hg–X interaction corresponds to a root-mean-square value for the variation in the distance of about 0.10 Å. For the X–X interaction, the corresponding value is about 0.24 Å. This can be compared to the mean amplitude of vibration calculated for $HgBr_3^-$ in TBP solution from observed vibrational frequencies, 0.0583 Å for Hg–Br and 0.1965 Å for Br–Br.[38]

Intermolecular interactions. The parameter values obtained for the HgX_n complexes were used to calculate peak shapes for the intramolecular Hg–X and X–X interactions, which were subtracted from the RDF's. The resulting functions (Fig. 7) indicate a remaining structure in the solutions, which cannot be explained by merely introducing a continuous electron contribution or a continuous complex distribution around each HgX_n complex.[16] Some of these remaining interactions occur at distances that are shorter than those expected for X–X contact distances. Thus, in HgX_4^{2-} solutions they can be explained only by contributions from X–H_2O or, to a smaller extent, from H_2O–H_2O and Na^+–H_2O interactions. It was found that a simple model for the packing of water molecules around an HgX_4^{2-} complex could account for most of these effects. A layer of water molecules, in an approximately close-packed arrangement (Fig. 6), was assumed to surround the HgX_4^{2-} complex. The distance of this layer from the center of the complex was refined in a least squares process, using appropriate parts of the reduced intensity curves. The halide-water distances obtained, Br^-–H_2O in the range 3.4 to 3.6 Å and I^-–H_2O 3.6 to 4.0 Å, are consistent with expected interatomic distances. The H_2O–H_2O distances within the layer could not, however, be separately adjusted, because their contributions to the intensity values were too small. The results of the refinement showed the long X–H_2O interactions to be much less distinct than the short ones. This indicates an arrangement in which the surrounding water molecules are in contact with the X atoms but do not have fixed positions on the surface of the HgX_4^{2-} complex.

The final model used to calculate theoretical intensities and RDF's consisted of an HgX_4^{2-} complex of tetrahedral symmetry or an HgX_3^- complex with an H_2O molecule in the fourth vertex, surrounded by a layer of water molecules (Fig. 6) outside of which the distribution of atoms was approximated by a continuous electron distribution. This is exemplified in Figs. 7 and 8 for the concentrated solution I2 (3.05 M Na_2HgI_4), where all water molecules as well as the sodium ions could be placed into this layer around the HgI_4^{2-} complex. The radius for the beginning of the even electron distribution, R = 5.06 Å, was estimated from the stoichiometric volume per Hg atom. For the more dilute solutions an average coordination of six water molecules around sodium and excess halide ions was also included. The contributions from residual water structure were approximated by assuming tetrahedral $(H_2O)_5$ groups.[39] An example is shown in Fig. 7 for the solution Br2 (1.63 M Na_2HgBr_4), where the radii chosen for the even electron distributions around the assumed species were 5.3 and 3.5 Å for the hydrated $HgBr_4^{2-}$ and Na^+ ions, and 3.2 Å for the H_2O groups, respectively.

Since the emergence of the continuum will not be sharp, a temperature factor, exp (-0.1 s^2), was included in all calculations.[39]

As shown in Fig. 7, this model approximately accounts for the observed interactions up to

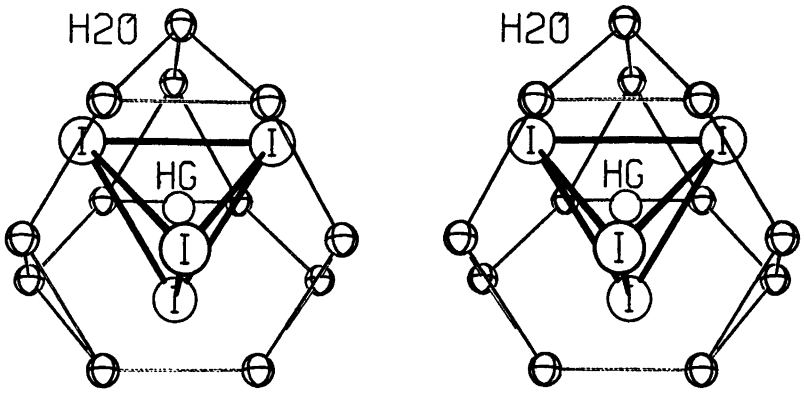

Fig. 6. The model used in the calculations for the packing of water molecules around an HgX_4^{2-} complex.

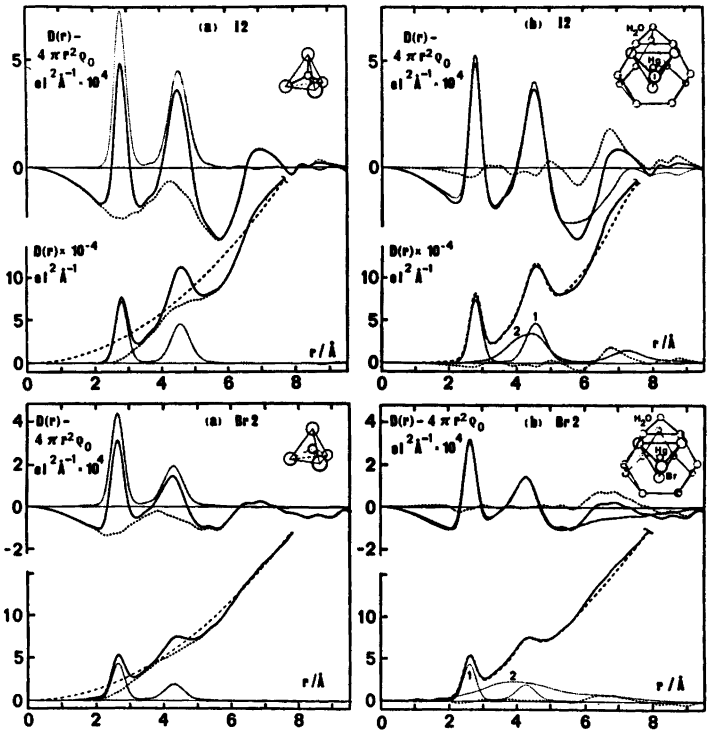

Fig. 7. Comparison between the experimental RDF's (solid lines) and (a) the peak shapes calculated for an HgX_4^{2-} tetrahedron (dotted lines), and (b) the calculated RDF's including both intra- and intermolecular interactions (dotted lines for the $D(r) - 4\pi r^2 \varrho_0$ functions and long dashes for the $D(r)$ curves). The dotted lines marked 1 are the peak shapes for an HgX_4^{2-} tetrahedron and those marked 2 represent the interactions between the HgX_4^{2-} complex and its surrounding hydration layer. For solution Br2 this curve 2 also contains the interactions within the assumed $Na(H_2O)_6^+$ and H_2O groups. The calculated RDF's also contain the contributions from an assumed even electron distribution around these species.

Differences between experimental and calculated curves are given by dashed lines (short dashes).

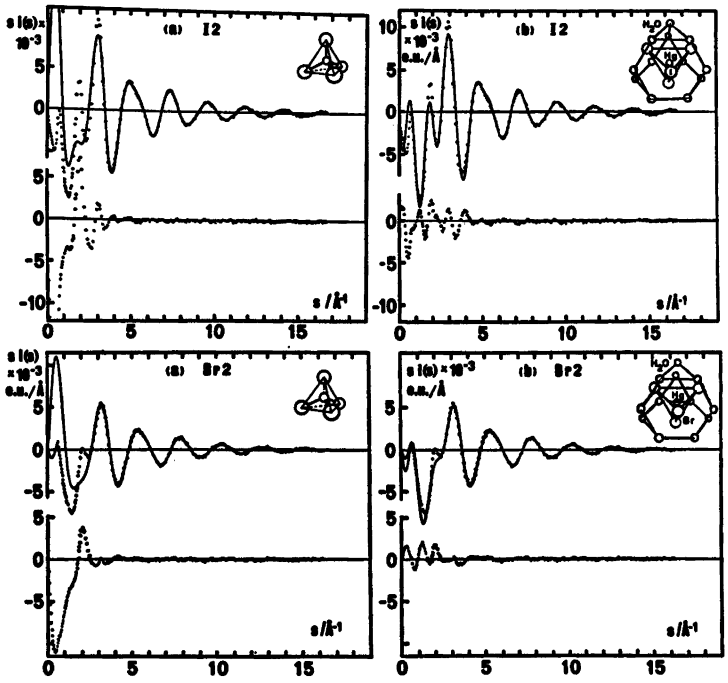

Fig. 8. Comparison between the experimental (dots) and calculated (solid lines) $si(s)$ values corresponding to the RDF's in Fig. 7.
The difference between experimental and calculated values is marked by dots below.

about 6 to 7 Å. The remaining interactions, which are too diffuse to allow an interpretation in terms of a specific structural model, probably result from the packing of the complexes not being completely random. This is supported by the observation that the remaining interactions become more pronounced as the concentration of the solution increases.

For the more concentrated solutions an attempt was made to relate the remaining interactions to possible restrictions in the free rotations of HgX_4^{2-} ions leading to preferred relative orientations of the groups. The model tried was based on the crystal structure of SnI_4, modified in a way similar to that used in the investigations of liquid CCl_4.[40] It became obvious, however, that such a model could not account for the observed interactions at the longer distances, and that the observed intermolecular interactions were too diffuse to be related to such a rigid model.

Conclusions and comparisons with other structure determinations. The bond lengths found for the HgI_4^{2-} and the $HgBr_4^{2-}$ complexes, 2.785(3) and 2.610(5) Å, respectively, are similar to values found for tetrahedrally coordinated mercury in crystal structures.[41–52] The comparatively low temperature factors obtained in the least squares refinements of the scattering data indicate that the Hg–X bond lengths in the aqueous solutions are more regular than is usually found in crystal structures.

The X-ray scattering data show, in an apparently conclusive way, that even in these concentrated solutions the HgI_3^- and the $HgBr_3^-$ complexes formed for X/Hg mol ratios <4, have no tendency to share X atoms which is in contrast to what is found in chloride solutions[2] and in the solid state where most mercury halides form infinite complexes[41–44,51–53] and few compounds have been found to contain discrete groups.[45–50,54]

Acknowledgements. The work has been supported by the Swedish Natural Science Research Council. Computer time was made available by the Computer Division of the National Swedish Office for Administrative Rationalization and Economy. We thank Mr. I. Duncan for linguistic help.

REFERENCES

1. Gaizer, F. and Johansson, G. *Acta Chem. Scand. 22* (1968) 3013.
2. Sandström, M. *Acta Chem. Scand. A 31* (1977) 141.
3. Sillén, L. G. and Martell, A. E. *Stability Constants*, Spec. Publ. No. 17 (1964) and *Suppl.* No. 1, Spec. Publ. No. 25, The Chemical Society, London 1971.
4. Deacon, G. B. *Rev. Pure Appl. Chem. 13* (1963) 189.
5. Sillén, L. G. *Acta Chem. Scand. 3* (1949) 539.
6. Arnek, R. *Ark. Kemi 24* (1965) 531.
7. van Panthaleon van Eck, C. L., Wolter, H. B. M. and Jaspers, W. J. M. *Recl. Trav. Chim. Pays-Bas 75* (1956) 802.
8. van Panthaleon van Eck, C. L. *Thesis*, Leiden 1958, see Gmelin *Handb. Anorg. Chem.* Hg-B2, Verlag Chemie Weinheim/Bergstr. 1967.
9. Furey, D. A. *Thesis*, Kent State University 1967 (Access No. 68-6207, Univ. Microfilms, Ann Arbor, Mich.).
10. Long, D. A. and Chau, J. Y. H. *Trans. Faraday Soc. 58* (1962) 2325.
11. Hooper, M. A. and James, D. W. *Aust. J. Chem. 24* (1971) 1345.
12. Macklin, J. W. and Plane, R. A. *Inorg. Chem. 9* (1970) 821.
13. Waters, D. N., Short, E. L., Tharwat, M. and Morris, D. F. C. *J. Mol. Struct. 17* (1973) 389.
14. Sandström, M. *To be published.*
15. Johansson, G. *Acta Chem. Scand. 25* (1971) 2787; *20* (1966) 553.
16. Johansson, G. and Sandström, M. *Chem. Scr. 4* (1973) 195.
17. Warren, B. E. and Mozzi, R. L. *Acta Crystallogr. 21* (1966) 459.
18. Cromer, D. T. and Waber, J. T. *Acta Crystallogr. 18* (1965) 104.
19. Stewart, R. F., Davidson, E. R. and Simpson, W. T. *J. Chem. Phys. 42* (1965) 3175.
20. Cromer, D. T. *Acta Crystallogr. 18* (1965) 17.
21. Cromer, D. T. *J. Chem. Phys. 50* (1969) 4857.
22. Compton, A. H. and Allison, S. K. *X-Rays in Theory and Experiment*, van Nostrand, New York 1935.
23. Cromer, D. T. and Mann, J. B. *J. Chem. Phys. 47* (1967) 1892.
24. Breit, G. *Phys. Rev. 27* (1926) 362.
25. Dirac, P. A. M. *Proc. R. Soc. London A 111* (1926) 405.
26. Dwiggins, C. W. and Park, D. A. *Acta Crystallogr. A 27* (1971) 264.
27. Narten, A. H. and Levy, H. A. *J. Chem. Phys. 55* (1971) 2263.
28. Sillén, L. G. *Acta Chem. Scand. 16* (1962) 159.
29. Warren, B. E. and Mozzi, R. L. *J. Appl. Crystallogr. 3* (1970) 59.
30. Milberg, M. E. *J. Appl. Phys. 29* (1958) 64.
31. Levy, H. A., Danford, M. D. and Narten, A. H. *Data Collection and Evaluation with an X-Ray Diffractometer Designed for the Study of Liquid Structure*, Report ORNL-3960, Oak Ridge National Laboratory, Oak Ridge 1966.
32. Pirenne, M. H. *The Diffraction of X-Rays and Electrons by Free Molecules*, Cambridge Univ. Press, London–New York 1946.
33. Åberg, M. *Acta Chem. Scand. 24* (1970) 2901.
34. Cromer, D. T. *Acta Crystallogr. 19* (1965) 224.
35. Warren, B. E. *X-Ray Diffraction*, Addison-Wesley, Reading, Massachusetts 1969.
36. Frey, M. and Monier, J. C. *Acta Crystallogr. B 27* (1971) 2487.
37. Leligny, H., Frey, M. and Monier, J. C. *Acta Crystallogr. B 28* (1972) 2104.
38. Sanyal, N. K., Goel, R. K. and Pandey, A. N. *Indian J. Phys. 49* (1975) 546.
39. Narten, A. H., Danford, M. D. and Levy, H. A. *Discuss. Faraday Soc. 43* (1967) 97, see also Luck, W., Ed., *Structure of Water and Aqueous Solutions*, Verlag Chemie, Weinheim/Bergstr. 1974.
40. Narten, A. H., Danford, M. D. and Levy, H. A. *J. Chem. Phys. 46* (1967) 4875.
41. Jeffrey, G. A. and Vlasse, M. *Inorg. Chem. 6* (1967) 397.
42. Hahn, H., Frank, G. and Klingler, W. *Z. Anorg. Allg. Chem. 279* (1955) 271.
43. Nyqvist, L. and Johansson, G. *Acta Chem. Scand. 25* (1971) 1615.
44. Fedorov, P. M. and Pakhomov, V. I. *Koord. Khim. 1* (1975) 1140.
45. Fedorov, P. M., Pakhomov, V. I. and Ivanova-Korfini, I. N. *Koord. Khim. 1* (1975) 1569.
46. Fenn, R. H. *Acta Crystallogr. 20* (1966) 24.
47. Fenn, R. H. *Acta Crystallogr. 20* (1966) 20.
48. Beurskens, P. T., Bosman, W. P. J. H. and Cras, J. A. *J. Cryst. Mol. Struct. 2* (1972) 183.
49. Harris, G. S., Inglis, F., McKechnie, J., Cheung, K. K. and Ferguson, G. *Chem. Commun. 9* (1967) 442.
50. Kamenar, B. and Nagl, A. *Acta Crystallogr. B 32* (1972) 1414.
51. Padmanabhan, V. M. and Ydava, V. S. *Acta Crystallogr. B 25* (1969) 647.
52. White, J. G. *Acta Crystallogr. 16* (1963) 397.
53. Brodersen, K. *Acta Crystallogr. 8* (1955) 723.

Received August 30, 1976.